

Published in final edited form as:

Biomaterials. 2007 June ; 28(18): 2821–2829. doi:10.1016/j.biomaterials.2007.02.024.

Requirement for Both Micron and Submicron Scale Structure for Synergistic Responses of Osteoblasts to Substrate Surface Energy and Topography

G. Zhao¹, A.L. Raines¹, M. Wieland², Z. Schwartz^{1,3}, and B.D. Boyan¹

¹Georgia Institute of Technology, Atlanta, Georgia, USA ²Institut Straumann AG, Basel, Switzerland

³Hebrew University Hadassah, Jerusalem, Israel

Abstract

Objective—Surface roughness and surface free energy are two important factors that regulate cell responses to biomaterials. Previous studies established that titanium substrates with micron-scale and submicron scale topographies promote osteoblast differentiation and osteogenic local factor production and that there is a synergistic response to microrough Ti surfaces that have retained their high surface energy via processing that limits hydrocarbon contamination. This study tested the hypothesis that the synergistic response of osteoblasts to these modified surfaces depends on both surface microstructure and surface energy.

Methods—Ti disks were manufactured to present three different surface structures: smooth pretreatment surfaces (PT) with R_a of 0.2 μm ; acid-etched surfaces (A) with a submicron roughness R_a of 0.83 μm ; and sandblasted/acid-etched surfaces (SLA) with R_a of 3–4 μm . Modified acid-etched (modA) and modified sandblasted/acid-etched (modSLA) titanium substrates, which have low contamination and present a hydroxylated/hydrated surface layer to retain high surface energy, were compared with regular low surface energy A and SLA surfaces. Human osteoblast-like MG63 cells were cultured on these substrates and their responses, including cell shape, growth, differentiation (alkaline phosphatase, osteocalcin), and local factor production (TGF- β 1, PGE₂, osteoprotegerin [OPG]) were analyzed (N=6 per variable). Data were normalized to cell number.

Results—There were no significant differences between smooth PT and A surfaces except for a small increase in OPG. Compared to A surfaces, MG63 cells produced 30% more osteocalcin on modA, and 70% more on SLA. However, growth on modSLA increased osteocalcin by more than 250%, which exceeded the sum of independent effects of surface energy and topography. Similar effects were noted when levels of latent TGF- β 1, PGE₂ and OPG were measured in the conditioned media.

Conclusions—The results demonstrate a synergistic effect between high surface energy and topography of Ti substrates and show that both micron scale and submicron scale structural features are necessary.

© 2007 Elsevier Ltd. All rights reserved.

Address for Correspondence Barbara D. Boyan, Ph.D., Department of Biomedical Engineering, Georgia Institute of Technology, 315 Ferst Drive NW, Atlanta, Georgia 30332-0363, Phone: 404-385-4108, FAX: 404-894-2291, E-mail: barbara.boyan@bme.gatech.edu .

Publisher's Disclaimer: This is a PDF file of an unedited manuscript that has been accepted for publication. As a service to our customers we are providing this early version of the manuscript. The manuscript will undergo copyediting, typesetting, and review of the resulting proof before it is published in its final citable form. Please note that during the production process errors may be discovered which could affect the content, and all legal disclaimers that apply to the journal pertain.

Keywords

Titanium; Surface energy; Microstructure; Submicron roughness; Osteoblast differentiation

INTRODUCTION

The surface properties of biomaterials determine the outcome of interactions between biomedical devices and the surrounding host tissue. The important surface properties involved in the process are chemical composition, topography, and energy. We and others have used titanium (Ti) as a model substrate for studying cell and tissue responses to biomaterials because of its clinical relevance, good biocompatibility and adaptability to diverse surface modifications [1–4]. Studies examining the contribution of surface micro-roughness show that differences in surface topography, including roughness, affect fibronectin and albumin adsorption in vitro [5], and growth of fibroblasts and osteoblast-like cells in culture [6]. Sandblasted Ti supports stronger osteoblast adhesion [7,8], related at least in part to altered integrin expression, higher focal contact density and reorganized cytoskeleton of cells on the rough surface [9]. Cells cultured on microrough Ti surfaces also exhibit decreased proliferation and increased differentiation [8,10]. Moreover, rough Ti surfaces increase osteoblast response to hormones and growth factors, including 1,25-dihydroxyvitamin D₃ [$1\alpha,25(\text{OH})_2\text{D}_3$], 17 β -estradiol and bone morphogenetic protein [11–13]. On rough Ti surfaces, osteoblasts also generate an osteogenic microenvironment to regulate bone remodeling, represented by releasing local factors to promote osteoblast differentiation and inhibit osteoclast activation [1]. These results are consistent with animal studies showing that Ti implants with greater roughness enhance bone-to-implant contact [14] and increase removal torque forces [15,16]. Clinical studies demonstrate that the preloading integration success rate of acid etched implants is significantly higher than seen with machined smooth implants [17].

Different surface modifications result in various surface roughness and topographies. For example, sandblasting produces micron scale roughness, but acid etching produces submicron scale roughness. The combination of these two methods results in a complicated three dimensional topography, which is similar to osteoclast resorption pits on bone wafers [18]. Studies using electron micro-machined surfaces show that micron scale roughness contributes to cell attachment, spreading and differentiation, and superposition of submicron scale enhances local factor production [19]. Moreover, osteoblasts are sensitive to the specific structural features of the superimposed roughness, exhibiting a more differentiated phenotype when the surface is created via acid etching rather than by anodic oxidation [20].

Surface energy is another important factor that regulates cell response to biomaterials. Pure Ti spontaneously grows an oxide layer with high surface energy. This oxide surface is hydrophilic because of binding structural water and forming -OH and -O²⁻ groups in its outermost layer. When in contact with electrolyte solutions, a surface film made of phosphate, titanium, calcium and hydroxyl groups spontaneously forms and nucleates an apatitic calcium phosphate layer [21]. Surface energy modulates protein adsorption, which further regulates cell adhesion, cell spreading and proliferation [22]. This can have consequences for the in vivo response to a material. Higher surface energy and increased wettability have been shown to enhance interaction between an implant surface and its biologic environment [23]. When implants with increased hydrophilicity are implanted in bone, the rate and extent of bone formation are increased, supporting the hypothesis that surface energy promotes bone cell maturation and differentiation [24].

While a biomaterial with higher surface energy is bioactive because of its reactive surface, a consequence is that it adsorbs inorganic anions or organic hydrocarbon contaminants from the

atmosphere within seconds to one minute. This results in an altered surface chemical composition and decreased hydrophilicity, potentially reducing the biological response. To solve this problem, a new processing method has been developed that retains the high surface energy of the uncontaminated TiO₂ surface by isolating it from contact with atmosphere. This modified sandblasted and acid etched TiO₂ (modSLA) is produced under the continuous protection of nitrogen, stored in isotonic solution and sterilized by gamma irradiation. Studies show that modSLA significantly increases human plasma fibronectin adsorption [25] and promotes osteoblast differentiation and activity in comparison with sandblasted and acid etched surfaces (SLA) produced under standard conditions [26]. In vivo studies show significantly increased bone-to-implant contact and enhanced angiogenesis on modSLA surfaces [27]. In addition, implants with modSLA surfaces provide high removal torque, indicating a higher stability during early stage of osseointegration [28].

The SLA surface has a complex topography consisting of craters varying in diameter from 30 to 100 μm overlaid with micropits varying in diameter from 1–3 μm . The micropit overlay results in an irregular distribution of sharply pointed projections approximately 700 nm in height, but because of the craters, the overall roughness is approximately 4 μm . Surface energy can be affected by roughness [29], but it is not known how surface energy regulates cell responses to different surface roughnesses if chemistry is held constant. To address this, we developed a model in which surface energy was held constant, but we varied surface microstructure. To do this, we prepared acid etched surfaces (A, modA) by the same protocols as are used to produce the acid etch on the SLA and modSLA substrates. These surfaces lacked the morphology generated by grit blasting, but had the same surface chemistry as the SLA and modSLA surfaces. The results of this study show that synergy between surface microtopography and surface energy requires both micron and submicron scale structural features.

METHODS

Substrates

Ti disks were prepared from 1 mm thick sheets of grade 2 unalloyed Ti (ASTM F67 “Unalloyed titanium for surgical implant applications”) and supplied to us by Institut Straumann AG (Basel, Switzerland). The disks were punched to be 15 mm in diameter so as to fit snugly into the well of a 24-well tissue culture plate. The methods used to produce the pretreatment (PT), SLA and modSLA surfaces have been reported previously [26]. PT is a smooth Ti surface with mean peak to valley roughness (R_a) of 0.2 μm . Submicron rough A surfaces were produced by treating PT with heated concentrated acid, resulting in an R_a of 830 nm, based on surface profilometry. PT surfaces were also sand blasted and acid etched to produce SLA surfaces with an R_a of 3.2 μm . Prior to use, PT, A, and SLA surfaces were washed in ultrasonic cleaner and sterilized in an oxygen plasma cleaner (PDC-32G, Harrick Plasma, Ithaca, NY). ModA and modSLA surfaces were produced with same mechanical or chemical treatments as A and SLA surfaces, respectively. However, the modA and modSLA surfaces were rinsed under nitrogen protection to prevent exposure to air during procedure, and then stored in a sealed glass tube containing isotonic NaCl solution. These sealed disks were sterilized by gamma irradiation at 25 kGy over night and ready for use.

Previous study showed that this treatment did not alter surface topography and roughness [26,30]. Instead this modification process changes surface chemical composition by decreasing carbon contamination by more than 50%, thereby retaining a higher surface energy. Rupp et al. [30] have published a detailed analysis of the A, modA, SLA, and modSLA surfaces. Advancing contact angles were used as an indicator for calculating surface free energy. Both A and SLA are very hydrophobic with water contact angles of 122.40° and 139.88°; in contrast, contact angles of modA and modSLA are close to 0°, indicating very hydrophilic surfaces.

Cell Culture

To compare cell responses to different surfaces properties, human osteoblast-like MG63 cells on tissue culture treated polystyrene (plastic) were compared to their morphology on the Ti substrates. MG63 cells were obtained from the American Type Culture Collection (Rockville, MD). The cells were cultured in Dulbecco's modified Eagle medium (DMEM) containing 10% fetal bovine serum (FBS) and 1% penicillin/streptomycin at 37°C in an atmosphere of 5% CO₂ and 100% humidity. Cells were plated at the same density of 10,000 cells/cm² tissue culture plastic for all surfaces. Media were exchanged at 24 hours and then every 48 hours until the cells reached confluence on plastic at day 6.

Cell Morphology

Cell morphology on the test surfaces was examined by LEO 1530 scanning electron microscopy (LEO Electron Microscopy, Oberkochen, Germany) at different time points (2, 4, 8 and 24 hours post-seeding and at 3 and 6 days). The cells were fixed with 2.5% glutaraldehyde in cacodylate buffer, dehydrated in a sequential series of ethanol followed by hexamethyl-disilazane, and then coated with gold.

Cell attachment on tissue culture polystyrene (TCPS) and Ti surfaces was evaluated by immunofluorescence staining. Cells were rinsed twice with phosphate buffered saline (PBS), and then fixed for 20 min in 4% paraformaldehyde followed by two PBS rinses. Cells were permeabilized with 0.1% Triton-X100 for 5 min at room temperature followed by two PBS rinses. Non-specific binding sites were blocked with 1% BSA in PBS (BSA/PBS) for 1 h. Cells were first incubated with mouse monoclonal anti-human vinculin antibody (MAB1674, Chemicon, Temecula, CA) (1:100 v/v) for 1 h at room temperature followed by a 1% BSA/PBS wash. The cells were then incubated with PBS containing rhodamine Red-X goat anti-mouse IgG (1:200 v/v), Alexa Fluor 488 Phalloidin (1:40 v/v) and Hoechst 33342 (1:10,000 v/v) (all from Molecular Probes, Eugene, Oregon) for 30 min, followed by three rinses with 0.05% Tween20/PBS. The Ti disks were mounted on a microscope slide under glass cover slips. The images were taken using a Nikon Eclipse E400 (Nikon Inc., Tokyo, Japan).

Cell Response

Cell number was determined in all cultures 24 hours after cells on tissue culture plastic reached confluence. Cells were released from the surfaces by two sequential incubations in 0.25% trypsin for 10 min at 37°C, in order to assure that any remaining cells were removed from rough TiO₂ surfaces. Released cells were counted using an automatic cell counter (Z1 cell and particle counter, Beckman Coulter, Fullerton, CA). Fewer than 1,000 cells were attached to the plastic surface underlying the Ti disks; therefore, these cells were not separated from total cells released from the disks, nor were they subtracted from the final cell numbers.

We used two determinants of osteoblast differentiation: alkaline phosphatase specific activity [orthophosphoric monoester phosphohydrolase, alkaline; E.C. 3.1.3.1] of cell lysates, and osteocalcin content of the conditioned media. Alkaline phosphatase is an early marker of differentiation and reaches its highest levels as mineralization is initiated. Osteocalcin is a late marker of differentiation and increases as mineral is deposited. Cell lysates were collected by centrifuging the cells after counting. Enzyme activity was assayed by measuring the release of *p*-nitrophenol from *p*-nitrophenylphosphate at pH 10.2 and results were normalized to protein content of the cell lysates [31]. The levels of osteocalcin in the conditioned media were measured using a commercially available radioimmunoassay kit (Human Osteocalcin RIA Kit, Biomedical Technologies, Stoughton, MA) and normalized to cell number, as described previously [11].

The conditioned media were also assayed for growth factors and cytokines. Osteoprotegerin (OPG) was measured using enzyme-linked immunosorbent assay (ELISA) kit (DY805 Osteoprotegerin DuoSet, R&D System, Minneapolis, MN). PGE₂ was assessed using a commercially available competitive binding radioimmunoassay kit (NEK020A Prostaglandin E₂ RIA kit, Perkin Elmer, Wellesley, MA). Active TGF- β 1 was measured prior to acidification of the conditioned media, using an ELISA kit specific for human TGF- β 1 (G7591 TGF- β 1 E_{max} Immunoassay System, Promega Corp., Madison, WI). Total TGF- β 1 was measured after acidifying the media and latent TGF- β 1 was defined as total TGF- β 1 minus active TGF- β 1 [11].

Statistical Analysis

The data presented here are from one of two separate sets of experiments. Both sets of experiments yielded comparable observations. For any given experiment, each data point represents the mean \pm standard error of six individual cultures. Data were first analyzed by analysis of variance; when statistical differences were detected, Student's *t*-test for multiple comparisons using Bonferroni's modification was used. *P*-values < 0.05 were considered to be significant.

RESULTS

The cells exhibited different shapes on PT, A and SLA surfaces. Scanning electron micrographs of the cells on the Ti substrates showed that at two hours after seeding, MG63 cells had become attached with a spherical morphology less than 10 μ m diameter (Fig. 1). Four hours after seeding, cells started to form extensions to explore the surface and the peripheral area of the cells flattened. By eight hours, the cells had become spread and had morphologies similar to those reaching confluence on plastic.

Kinetic immunofluorescence micrographs (Fig. 2) confirmed these observations and provided information concerning the cytoskeleton of the cells during attachment and spreading. Cells changed shape as a function of time following attachment in a surface dependent manner. Two hours after seeding, the cells had a round morphology on all surfaces except PT. Most cells exhibited one or two red spots with strong intensity, representing vinculin accumulations at the beginning of cell attachment. Actin was not distributed evenly in the cells; instead most of the actin was assembled at one side of the nucleus. At four hours after seeding, the cells on relatively smooth surfaces (TCPS, PT and A) had begun to spread. Cells on the rough SLA surfaces were beginning to form lamellipodia, but not to the same extent as seen on smooth surfaces. In contrast, MG63 cells on high energy surfaces (modA and modSLA) did not exhibit significant shape changes at 4 h. At 8 hours after seeding, cells on PT, A and SLA continued to spread and exhibited a bi-polar or spindle-like shape through the first 24 hours. The spreading of cells on high energy surfaces (modA and modSLA) was slower than seen on hydrophobic surfaces. Because of surface roughness, parts of the images on the SLA and modSLA surfaces were out of the plane of focus.

Scanning electron microscopy was also able to discern substrate-dependent differences in the shape of individual cells in higher density cultures (Fig. 1), which could not be resolved using immunofluorescence. Cells increased in number on all surfaces between days 1 to 6. MG63 cells on PT surfaces in general were flat and had two or three major extensions. On A and modA, the cells were elongated and formed spindle-like shapes. On SLA and modSLA, the cells were polygonal in shape with many thin filopodia attached to the surfaces.

After 6 days of in vitro culture, the MG63 cells reached confluence on plastic surfaces. Cell number on PT and A surfaces were the same as those on tissue culture plastic, indicating that submicron roughness on flat Ti surface had no effect on cell number (Fig. 3). Cell number on

the SLA surface, which presents a combination of micron and submicron structures, decreased by 44% compared to smooth PT. By comparing modA and A surfaces, high surface energy decreased cell number by 25%. However, in the presence of a complicated three dimensional topography like SLA, higher surface energy decreased cell number by almost 50%.

Cells cultured on all Ti surfaces exhibited decreased alkaline phosphatase activity compared to those on plastic (Fig. 4A). Although the enzyme activity of cells on SLA was 30% less than that on PT, there was no statistical difference among PT, A, modA and SLA surfaces. With higher surface energy on modSLA, enzyme activity was 60% lower than on SLA.

Osteocalcin levels in cultures grown on PT and A were the same as on plastic (Fig. 4B). With high surface energy on submicron scale roughness, osteocalcin levels in cultures grown on modA increased by 30% compared with cultures grown on A. The micron roughness of SLA increased osteocalcin by 70% compared to A. There was as strong synergistic effect between surface energy and roughness. The combination of high surface energy and micron-scale roughness enhanced osteocalcin by more than 250%.

Local factors were also regulated by surface properties. OPG levels increased on all Ti surfaces except smooth PT (Fig. 5A). OPG in the conditioned media of cells grown on modA was slightly higher (20%) than on A, but the difference is not statistically significant. Compared with cultures grown on A, OPG on SLA increased 50% with statistic significance. The amount of OPG was almost doubled on modSLA surfaces, showing a synergistic effect of surface high energy and micron structure on osteoprotegerin production. PGE₂ was affected in a similar manner (Fig. 5B). The degree of PGE₂ enhancement on modSLA (600%) was more than the combination of the increase on modA (100%) and SLA (200%). Active TGF- β 1 was unaffected by the surface. However, latent TGF- β 1 was modulated in a surface-specific manner, with a 120% increase on SLA and a 330% increase on modSLA. Moreover, latent TGF- β 1 levels in conditioned media of cells cultured on modSLA was 65% greater than in the media of cells grown on SLA.

DISCUSSION

The results of this study show that high surface energy is an important variable but by itself it is insufficient to cause marked increases in osteoblast responses to Ti substrates with low surface roughness. In contrast, when substrates with complex micron scale and submicron scale roughness are fabricated to retain the high surface energy of uncontaminated TiO₂, the cells exhibit synergistic enhancement of their response to the surface topography alone. This includes reduced cell number together with increased differentiation and release of factors into the media that stimulate osteogenesis and reduce osteoclastic activity.

Scanning electron microscopic analysis and immunofluorescence of cell morphology identified significant differences in cell shape as a function of both surface chemistry and surface topography, confirming our previous work and the work of others [32,33]. Immunofluorescence images of MG63 cells over the first 24 hours after seeding demonstrated that osteoblasts on smooth and low energy surfaces spread faster than those on rough and higher energy surfaces. Scanning electron micrographs showed that differences in cell shape were retained even after cell density increased. MG63 cells on PT surfaces, like those on plastic, in general were flat and had two or three major extensions. On A and modA, the cells were elongated and formed spindle like shape; on SLA and modSLA, the cells were polygonal in shape with many thin filopodia to attach to the surfaces.

The observation that osteoblasts grown on smooth Ti surface had fewer cytoplasmic extensions than cells grown on micron and submicron structured surfaces, is consistent with previous findings [8,34]. Although both A and SLA surfaces had similar 1–2 μ m pits produced by acid

etching, the MG63 cells grown on SLA extended many more filopodia to attach themselves to the substrates. This suggests that the cells not only sense direct focal contacts with the substrate, but they also respond to the broader waviness created by sand blasting. Others have reported comparable effects of surface topography on epithelial cells [35], suggesting that this is a general property of cell interactions with surface microarchitecture.

Our results confirmed our previous findings that submicron scale roughness, while contributing to the overall response of the cells, is not a major determinant of cell behavior in the absence of the larger craters [20]. In the present study, with the exception of OPG production, growth on A did not alter osteoblast number, differentiation or local factor levels to any great extent in comparison with growth on the PT surface. However, in combination with micron scale roughness, typified by SLA, there were significant increases in local factor levels to produce an osteogenic environment [20]. This phenomenon may be due to interference between surface topography and surface energy. The potential effect of submicron scale roughness is counteracted by lower surface energy. Other researchers have observed that osteoblasts grown on nano-textured surfaces express higher osteopontin and bone sialoprotein [36]. Full characterization of surface energy along with surface roughness is necessary to understand cell/substrate interactions.

Our results show a strong synergistic effect between micron scale roughness and surface energy. When MG63 cells were grown on A and modA substrates, the increase in surface energy had no effect on alkaline phosphatase activity or latent TGF- β 1 levels, and only a small increase in osteocalcin or PGE₂. In contrast, when the surface presented a complicated micron scale roughness, increased surface energy greatly decreased cell number and enhanced cell differentiation by more than 100%. Both modA and modSLA were produced using the same acid etching procedure to ensure the same surface chemistry. Therefore the differences observed in the cell response were only dependent on micron scale roughness. We did not include modified PT substrates to examine the effect of high surface energy on a relatively smooth surface because PT surfaces were mechanically machined and chemically degreased, resulting in a final modified PT surface chemistry that would be different from modA or modSLA.

It is likely that the differential response of MG63 cells to surface roughness and topography reflects differences in integrin mediated signaling. Cells respond to biomaterial surfaces through interaction between plasma membrane receptor integrins and adsorbed extracellular matrix proteins including fibronectin [37]. Protein adsorption is highly influenced by surface chemistry, hydrophilicity and topography; small proteins tend to adsorb on hydrophobic surfaces, but large proteins are less affected by surface wettability [38]. In addition, proteins adsorbed onto hydrophobic surfaces are more sensitive to unfolding and denaturing processes due to electrostatic forces between the surface and cells. Thus, fibronectin fragments adsorb faster on hydrophobic -CH₃ surfaces, but lack cell adhesion activity [39]. Protein adsorption also depends on the scale of surface roughness. Nano scale surface texture seems have little to no effect on protein adsorption and cell proliferation [40]. However, microrough surfaces adsorb more fibronectin and the protein orientation is different from that on machined smooth Ti, which further alters integrin adhesion. In addition, the profile of integrin expression in osteoblasts is sensitive to surface roughness [9]. These findings indicate cell behavior is not determined by a single surface feature, but is in response to combinations of different surface properties as a whole.

Previous studies show that osteoblasts grown on microrough surfaces produce an osteogenic environment to promote osteoblast differentiation by paracrine and autocrine pathways [1]. Our results suggest that the increase in the rate and extent of peri-implant bone formation seen with modSLA implants in vivo [27] reflects enhanced osteogenesis as well. Osteocalcin levels

were increased whereas alkaline phosphatase specific activity was decreased, indicative of mature secretory osteoblasts [41]. PGE₂, which is necessary for osteoblastic differentiation [1], was also increased. Interestingly, levels of OPG, a local factor produced by osteoblasts that reduces osteoblast-dependent activation of osteoclasts [42], were higher as well. These results indicate that the increase of OPG on modSLA surfaces plays an important role in controlling osteoclast differentiation in bone remodeling cycle, and contributes to early upregulation of bone to implant contact [27].

TGF- β 1 also reduces osteoclast activity [43] and increases osteoblast differentiation [44]. We previously showed that cells grown on SLA deposit more TGF- β 1 in their extracellular matrix than do cells grown on smooth Ti [45], and cells grown on modSLA release increased levels of latent TGF- β 1 into their media than do cells grown on SLA. In the present study, we also found higher levels of latent growth factor in the conditioned media of cells grown on SLA and this was further increased when cells were cultured on modSLA. This suggests that cells on the more reactive surface are producing a larger reservoir of growth factors on high energy surfaces that can be used downstream to control osteoclast formation and activity.

CONCLUSION

In summary, this study examined the independent effect of surface roughness and surface energy by applying a modification technique to eliminate hydrophobic surface contamination and retain a high surface energy. Osteoblast-like cells cultured on higher energy surfaces exhibit a more differentiated phenotype and produce more local factors to regulate osteoblast and osteoclast activity. The combination of micron scale roughness and high surface energy synergistically promotes osteoblast responses. The results suggest that surface energy is an important factor in mediating cell-substrate interactions, and higher surface energy should be incorporated in biomaterial design to improve the host tissue response.

ACKNOWLEDGMENTS

The authors thank Institut Straumann AG (Basel, Switzerland) for providing the Ti disks used in this study. The research was supported by a grant from the ITI Foundation (Basel, Switzerland), the NSF (EEC 9731643) and NIH (AR052102). The authors would like to thank Dr. F. Rupp and Prof. J. Geis-Gerstorfer, Dental Clinic, Department of Prosthodontics, Section of Medical Materials & Technology, 72076 Tübingen, Germany, for providing us with their thorough characterization of the physical and chemical properties of the A and modA surfaces. These analyses are now published [30].

REFERENCES

1. Boyan BD, Lissdorfer S, Wang L, Zhao G, Lohmann CH, Cochran DL, Schwartz Z. Osteoblasts generate an osteogenic microenvironment when grown on surfaces with rough microtopographies. *Eur Cell Mater* 2003;6:22–27. [PubMed: 14577052]
2. Pohler OE. Unalloyed titanium for implants in bone surgery. *Injury* 2000;31:7–13. [PubMed: 11270082]
3. Cooper LF. A role for surface topography in creating and maintaining bone at titanium endosseous implants. *J Prosthet Dent* 2000;84:522–534. [PubMed: 11105008]
4. Puleo DA, Nanci A. Understanding and controlling the bone-implant interface. *Biomaterials* 1999;20:2311–2321. [PubMed: 10614937]
5. Francois P, Vaudaux P, Taborelli M, Tonetti M, Lew DP, Descouts P. Influence of surface treatments developed for oral implants on the physical and biological properties of titanium. (II) Adsorption isotherms and biological activity of immobilized fibronectin. *Clin Oral Implants Res* 1997;8:217–225. [PubMed: 9586466]
6. Harris LG, Patterson LM, Bacon C, Gwynn I, Richards RG. Assessment of the cytocompatibility of different coated titanium surfaces to fibroblasts and osteoblasts. *J Biomed Mater Res A* 2005;73:12–20. [PubMed: 15704113]

7. Keller JC, Schneider GB, Stanford CM, Kellogg B. Effects of implant microtopography on osteoblast cell attachment. *Implant Dent* 2003;12:175–181. [PubMed: 12861887]
8. Martin JY, Schwartz Z, Hummert TW, Schraub DM, Simpson J, Lankford J, Dean DD, Cochran DL, Boyan BD. Effect of Titanium Surface-Roughness on Proliferation, Differentiation, and Protein-Synthesis of Human Osteoblast-Like Cells (MG63). *J Biomed Mater Res* 1995;29:389–401. [PubMed: 7542245]
9. Raz P, Lohmann CH, Turner J, Wang L, Poythress N, Blanchard C, Boyan BD, Schwartz Z. 1 α , 25(OH)2D3 regulation of integrin expression is substrate dependent. *J Biomed Mater Res A* 2004;71A: 217–225. [PubMed: 15386491]
10. Brunette DM. The effects of implant surface topography on the behavior of cells. *Int J Oral Maxillofac Implants* 1988;3:231–246. [PubMed: 3075965]
11. Boyan BD, Batzer R, Kieswetter K, Liu Y, Cochran DL, Szmuckler-Moncler S, Dean DD, Schwartz Z. Titanium surface roughness alters responsiveness of MG63 osteoblast-like cells to 1 α , 25-(OH)(2)D-3. *J Biomed Mater Res* 1998;39:77–85. [PubMed: 9429099]
12. Ong JL, Carnes DL, Cardenas HL, Cavin R. Surface roughness of titanium on bone morphogenetic protein-2 treated osteoblast cells in vitro. *Implant Dent* 1997;6:19–24. [PubMed: 9206401]
13. Lohmann CH, Tandy EM, Sylvia VL, Hell-Vocke AK, Cochran DL, Dean DD, Boyan BD, Schwartz Z. Response of normal female human osteoblasts (NHOb) to 17 beta-estradiol is modulated by implant surface morphology. *J Biomed Mater Res* 2002;62:204–213. [PubMed: 12209940]
14. Buser D, Schenk RK, Steinemann S, Fiorellini JP, Fox CH, Stich H. Influence of surface characteristics on bone integration of titanium implants. A histomorphometric study in miniature pigs. *J Biomed Mater Res* 1991;25:889–902. [PubMed: 1918105]
15. Wennerberg A, Ektessabi A, Albrektsson T, Johansson C, Andersson B. A 1-year follow-up of implants of differing surface roughness placed in rabbit bone. *Int J Oral Maxillofac Implants* 1997;12:486–494. [PubMed: 9274077]
16. Klokkevold PR, Nishimura RD, Adachi M, Caputo A. Osseointegration enhanced by chemical etching of the titanium surface. A torque removal study in the rabbit. *Clin Oral Implants Res* 1997;8:442–447. [PubMed: 9555202]
17. Khang W, Feldman S, Hawley CE, Gunsolley J. A multi-center study comparing dual acid-etched and machined-surfaced implants in various bone qualities. *J Periodontol* 2001;72:1384–1390. [PubMed: 11699480]
18. Boyan BD, Schwartz Z, Lohmann CH, Sylvia VL, Cochran DL, Dean DD, Puzas JE. Pretreatment of bone with osteoclasts affects phenotypic expression of osteoblast-like cells. *J Orthop Res* 2003;21:638–647. [PubMed: 12798063]
19. Zinger O, Zhao G, Schwartz Z, Simpson J, Wieland M, Landolt D, Boyan B. Differential regulation of osteoblasts by substrate microstructural features. *Biomaterials* 2005;26:1837–1847. [PubMed: 15576158]
20. Zhao G, Zinger O, Schwartz Z, Wieland M, Landolt D, Boyan BD. Osteoblast-like cells are sensitive to submicron-scale surface structure. *Clin Oral Implants Res* 2006;17:258–264. [PubMed: 16672020]
21. Li P, Ohtsuki C, Kokubo T, Nakanishi K, Soga N, de Groot K. The role of hydrated silica, titania, and alumina in inducing apatite on implants. *J Biomed Mater Res* 1994;28:7–15. [PubMed: 8126031]
22. Kennedy SB, Washburn NR, Simon CG Jr, Amis EJ. Combinatorial screen of the effect of surface energy on fibronectin-mediated osteoblast adhesion, spreading and proliferation. *Biomaterials* 2006;27:3817–3824. [PubMed: 16563495]
23. Baier RE, Meyer AE, Natiella JR, Natiella RR, Carter JM. Surface properties determine bioadhesive outcomes: methods and results. *J Biomed Mater Res* 1984;18:327–355. [PubMed: 6736072]
24. Eriksson C, Nygren H, Ohlson K. Implantation of hydrophilic and hydrophobic titanium discs in rat tibia: cellular reactions on the surfaces during the first 3 weeks in bone. *Biomaterials* 2004;25:4759–4766. [PubMed: 15120522]
25. Scheideler, L.; Rupp, F.; Wieland, M.; Geis-Gerstorfer, J. Storage Conditions of Titanium Implants Influence Molecular and Cellular Interactions; 83rd General Session and Exhibition of the International Association for Dental Research; 2006. Poster # 870

26. Zhao G, Schwartz Z, Wieland M, Rupp F, Geis-Gerstorfer J, Cochran DL, Boyan BD. High surface energy enhances cell response to titanium substrate microstructure. *J Biomed Mater Res A* 2005;74:49–58. [PubMed: 15924300]
27. Buser D, Broggini N, Wieland M, Schenk RK, Denzer AJ, Cochran DL, Hoffmann B, Lussi A, Steinemann SG. Enhanced Bone Apposition to a Chemically Modified SLA Titanium Surface. *J Dent Res* 2004;83:529–533. [PubMed: 15218041]
28. Ferguson SJ, Broggini N, Wieland M, de WM, Rupp F, Geis-Gerstorfer J, Cochran DL, Buser D. Biomechanical evaluation of the interfacial strength of a chemically modified sandblasted and acid-etched titanium surface. *J Biomed Mater Res A* 2006;78:291–297. [PubMed: 16637025]
29. Rupp F, Scheideler L, Rehbein D, Axmann D, Geis-Gerstorfer J. Roughness induced dynamic changes of wettability of acid etched titanium implant modifications. *Biomaterials* 2004;25:1429–1438. [PubMed: 14643618]
30. Rupp F, Scheideler L, Olshanska N, de WM, Wieland M, Geis-Gerstorfer J. Enhancing surface free energy and hydrophilicity through chemical modification of microstructured titanium implant surfaces. *J Biomed Mater Res A* 2006;76:323–334. [PubMed: 16270344]
31. Bretau diere JP, Spillman T. Alkaline phosphatases. 1984:75–92.
32. Ismail FS, Rohanizadeh R, Atwa S, Mason RS, Ruys AJ, Martin PJ, Bendavid A. The influence of surface chemistry and topography on the contact guidance of MG63 osteoblast cells. *J Mater Sci Mater Med*. 2006
33. Goto T, Yoshinari M, Kobayashi S, Tanaka T. The initial attachment and subsequent behavior of osteoblastic cells and oral epithelial cells on titanium. *Biomed Mater Eng* 2004;14:537–544. [PubMed: 15472400]
34. Zhu X, Chen J, Scheideler L, Altebaeumer T, Geis-Gerstorfer J, Kern D. Cellular reactions of osteoblasts to micron- and submicron-scale porous structures of titanium surfaces. *Cells Tissues Organs* 2004;178:13–22. [PubMed: 15550756]
35. Di CM, Toto P, Feliciani C, Scarano A, Tulli A, Strocchi R, Piattelli A. Spreading of epithelial cells on machined and sandblasted titanium surfaces: an in vitro study. *J Periodontol* 2003;74:289–295. [PubMed: 12710747]
36. de Oliveira PT, Nanci A. Nanotexturing of titanium-based surfaces upregulates expression of bone sialoprotein and osteopontin by cultured osteogenic cells. *Biomaterials* 2004;25:403–413. [PubMed: 14585688]
37. Degasne I, Basle MF, Demais V, Hure G, Lesourd M, Grolleau B, Mercier L, Chappard D. Effects of roughness, fibronectin and vitronectin on attachment, spreading, and proliferation of human osteoblast-like cells (Saos-2) on titanium surfaces. *Calcif Tissue Int* 1999;64:499–507. [PubMed: 10341022]
38. Sigal GB, Mrksich M, Whitesides GM. Effect of surface wettability on the adsorption of proteins and detergents. *Journal of the American Chemical Society* 1998;120:3464–3473.
39. Michael KE, Vernekar VN, Keselowsky BG, Meredith JC, Latour RA, Garcia AJ. Adsorption-induced conformational changes in fibronectin due to interactions with well-defined surface chemistries. *Langmuir* 2003;19:8033–8040.
40. Cai K, Bossert J, Jandt KD. Does the nanometre scale topography of titanium influence protein adsorption and cell proliferation? *Colloids Surf B Biointerfaces* 2006;49:136–144. [PubMed: 16621470]
41. Stein GS, Lian JB, Owen TA. Relationship of cell growth to the regulation of tissue-specific gene expression during osteoblast differentiation. *FASEB J* 1990;4:3111–3123. [PubMed: 2210157]
42. Lacey DL, Timms E, Tan HL, Kelley MJ, Dunstan CR, Burgess T, Elliott R, Colombero A, Elliott G, Scully S, Hsu H, Sullivan J, Hawkins N, Davy E, Capparelli C, Eli A, Qian YX, Kaufman S, Sarosi I, Shalhoub V, Senaldi G, Guo J, Delaney J, Boyle WJ. Osteoprotegerin ligand is a cytokine that regulates osteoclast differentiation and activation. *Cell* 1998;93:165–176. [PubMed: 9568710]
43. Bonewald LF, Mundy GR. Role of transforming growth factor-beta in bone remodeling. *Clin Orthop Relat Res* 1990:261–276. [PubMed: 2403492]
44. Bonewald LF, Kester MB, Schwartz Z, Swain LD, Khare A, Johnson TL, Leach RJ, Boyan BD. Effects of combining transforming growth factor beta and 1,25-dihydroxyvitamin D3 on

- differentiation of a human osteosarcoma (MG-63). *J Biol Chem* 1992;267:8943–8949. [PubMed: 1577731]
45. Kieswetter K, Schwartz Z, Hummert TW, Cochran DL, Simpson J, Dean DD, Boyan BD. Surface roughness modulates the local production of growth factors and cytokines by osteoblast-like MG-63 cells. *J Biomed Mater Res* 1996;32:55–63. [PubMed: 8864873]

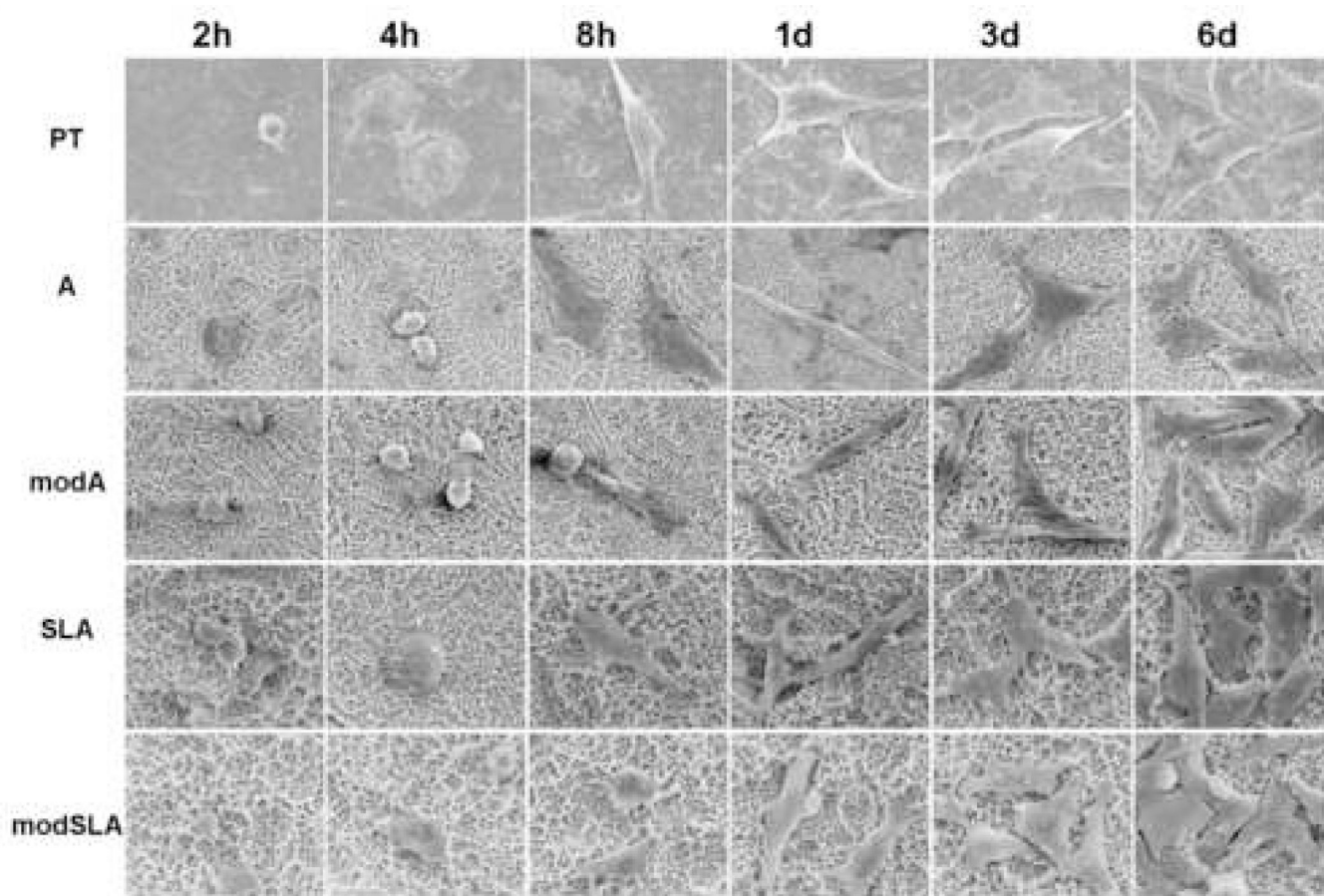


Figure 1.

Morphology of MG63 osteoblast-like cells cultured on Ti surfaces. MG63 cells were grown on PT, A, modA, SLA and modSLA surfaces for 2 h, 4 h, 8 h, 1 d, 3 d and 6 d and their morphology imaged by scanning electron microscopy. Areas of lower cell density were selected to facilitate observation of individual cell shapes. The images of the cells shown in the selected micrographs are typical of cells throughout the culture.

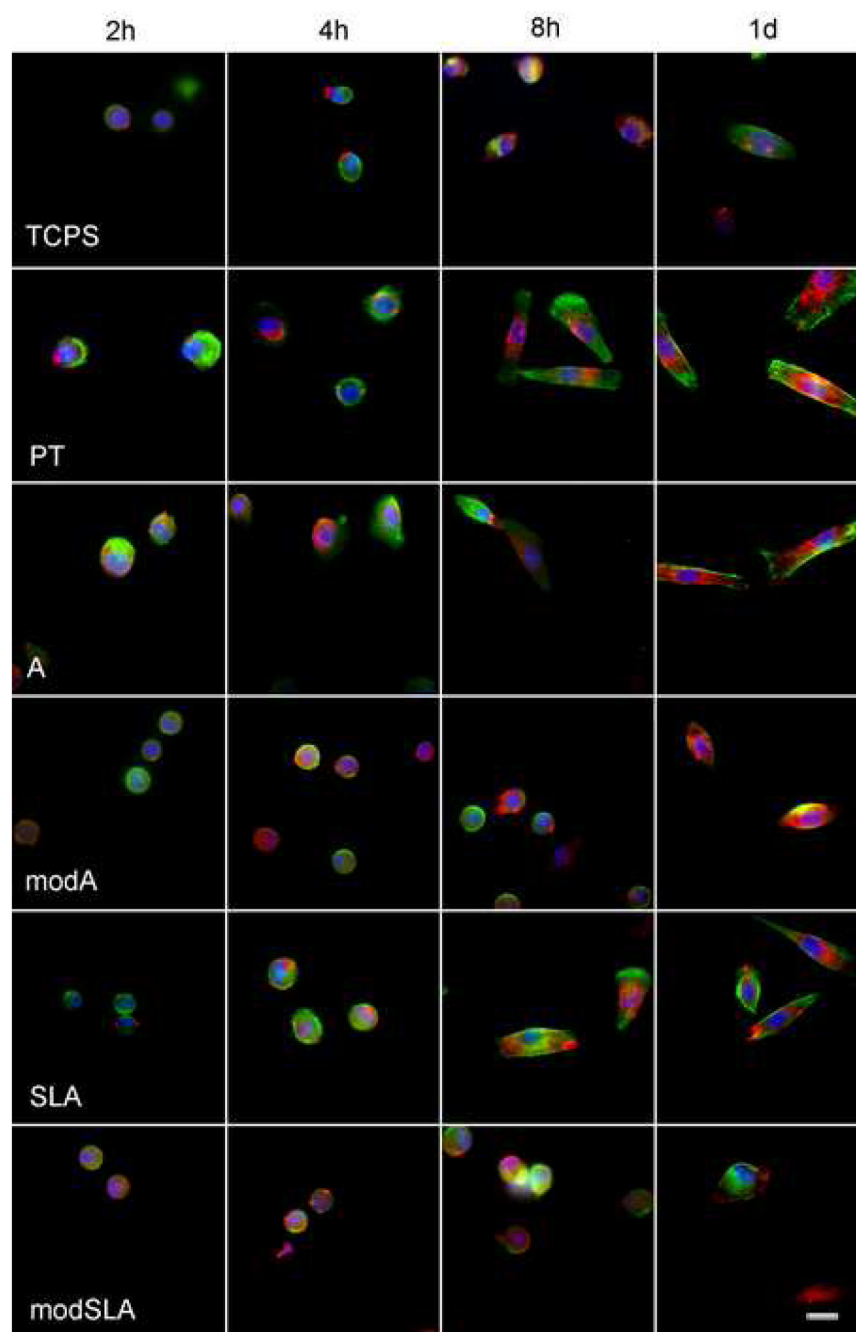


Figure 2.

Immunofluorescent staining of MG63 cells cultured on tissue culture polystyrene (TCPS) and Ti surfaces. MG63 cells were seeded on TCPS, PT, A, modA, SLA and modSLA surfaces for 2, 4, 8, and 24 hours. Cells were stained for vinculin (red), actin (green) and nucleus (blue). The yellow color represents the co-localization of vinculin and actin. Scale bar = 20 μ m.

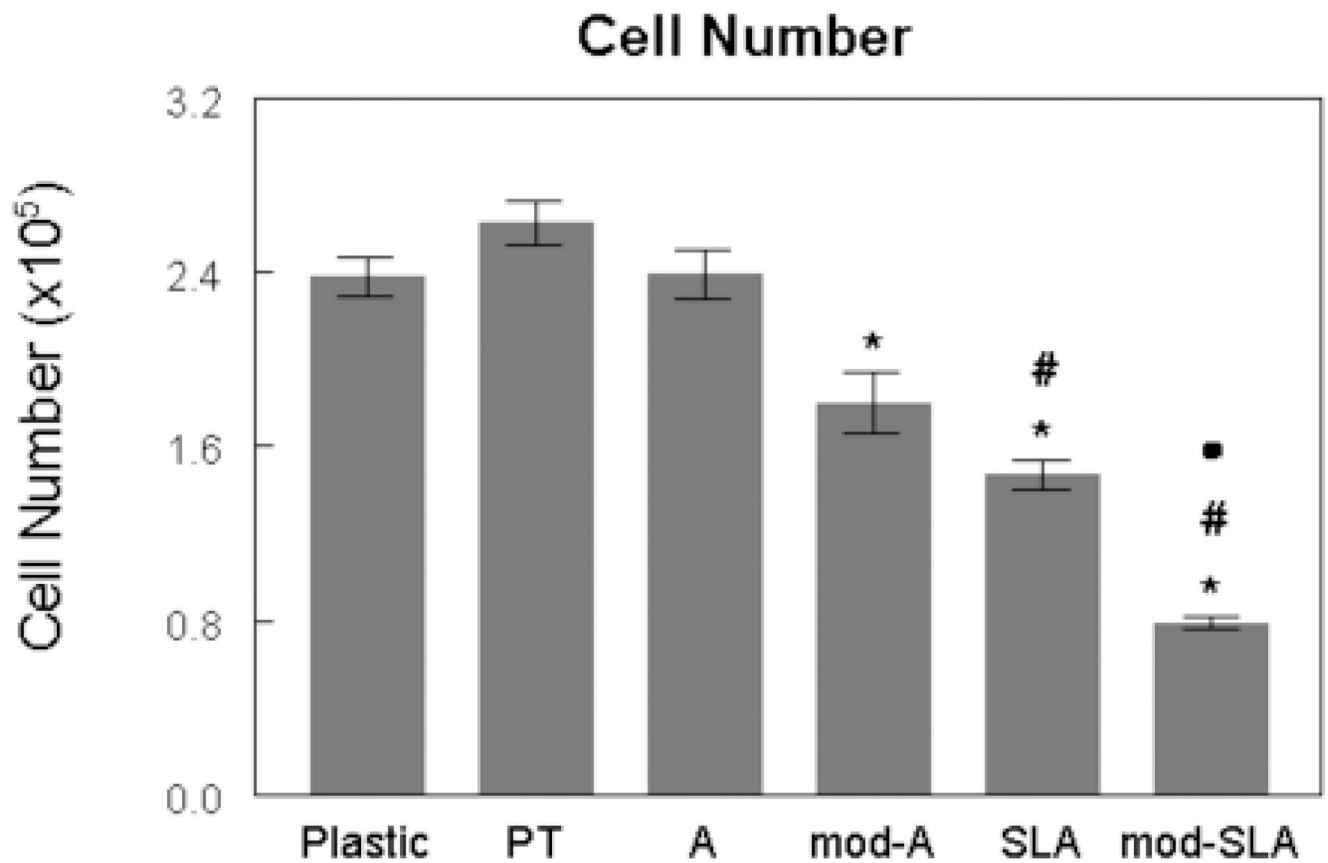


Figure 3.

Effect of surface microstructure and surface energy on cell number. MG63 cells were cultured on tissue culture polystyrene (plastic), PT, A, mod A, SLA and modSLA surfaces. Cell number was determined 24-hours after cells reached confluence on plastic surfaces. Values are means + SEM of six independent cultures. Data are from one of two separate experiments, both with comparable results. Data were analyzed by ANOVA and significant differences between groups determined using the Bonferroni modification of Student's t-test. * $p < 0.05$, Ti surfaces v. plastic; # $p < 0.05$, v. PT; • $p < 0.05$, v. SLA surface.

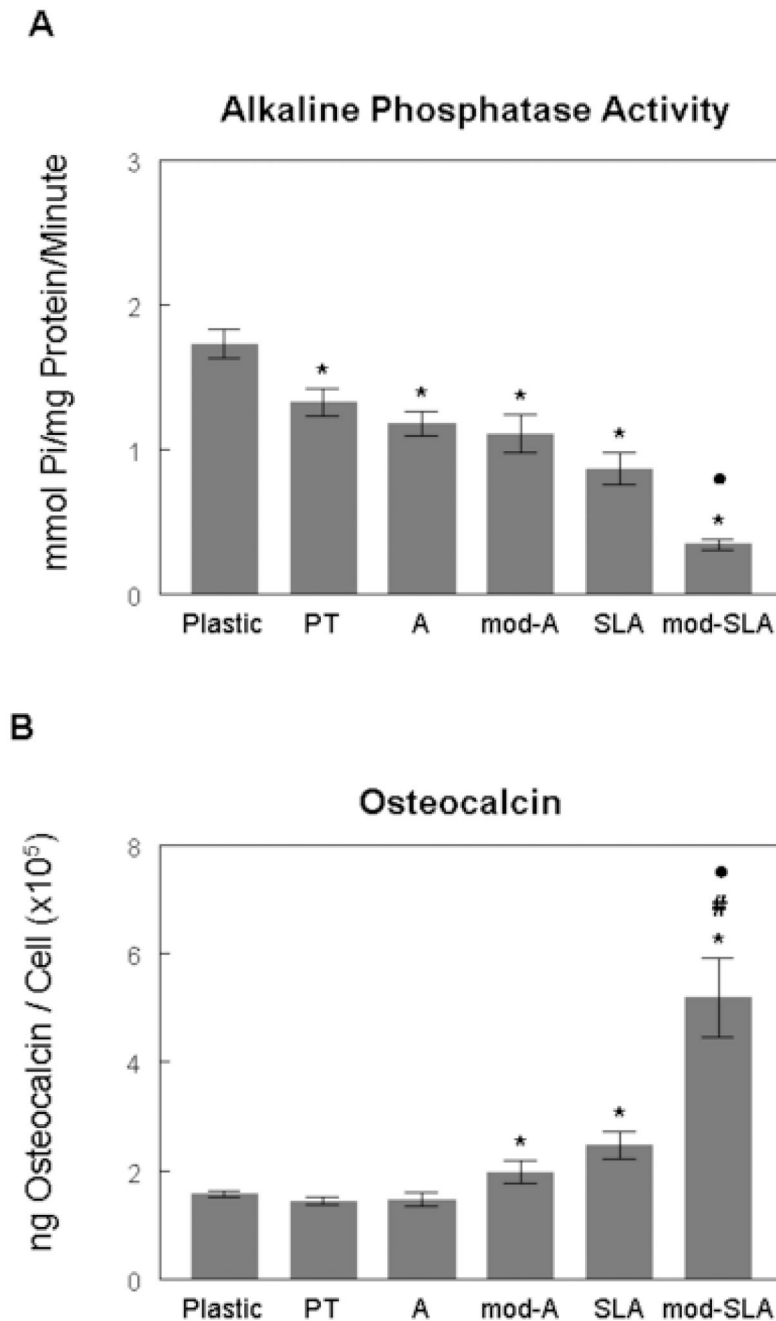


Figure 4.

Effect of surface microstructure and surface energy on cell differentiation. MG63 cells were cultured on tissue culture polystyrene (plastic), PT, A, mod A, SLA and modSLA surfaces. (A) Alkaline phosphatase specific activity was measured in isolated cells. (B) Osteocalcin levels were measured in conditioned media of confluent cultures. Values are means \pm SEM of six independent cultures. Data are from one of two separate experiments, both with comparable results. Data were analyzed by ANOVA and significant differences between groups determined using the Bonferroni modification of Student's t-test. * $p < 0.05$, Ti surfaces v. plastic; # $p < 0.05$, v. A; • $p < 0.05$, v. SLA surface.

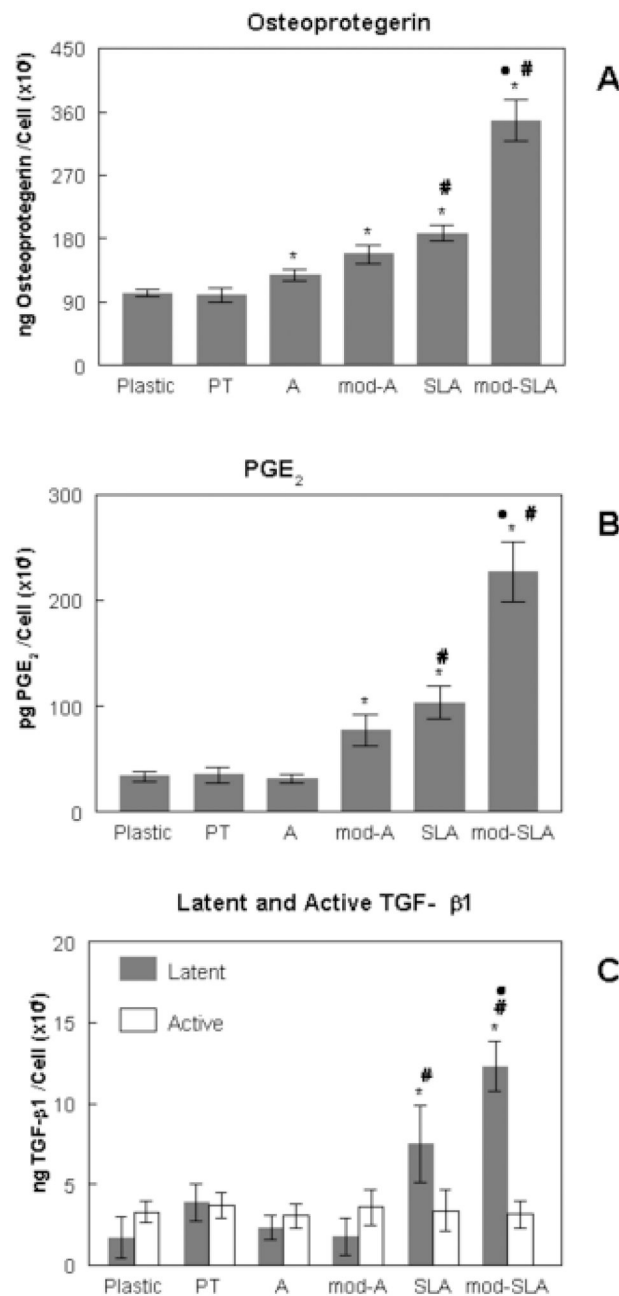


Figure 5.

Effect of surface microstructure and surface energy on local factor levels. MG63 cells were cultured on tissue culture polystyrene (plastic), PT, A, mod A, SLA and modSLA surfaces. (A) Osteoprotegerin levels of conditioned media were determined by ELISA kit. (B) PGE₂ contents of the conditioned media were determined by RIA. Active TGF-β1 and latent TGF-β1 (C) in the conditioned media were measured using an ELISA kit. Values are means ± SEM of six independent cultures. Data are from one of two separate experiments, both with comparable results. Data were analyzed by ANOVA and significant differences between groups determined using the Bonferroni modification of Student's t-test. *p<0.05, Ti surfaces v. plastic; #p<0.05, v. A; •p<0.05, v. SLA surface.